Performances of Microwave Photonic Notch Filter Based on Microring Resonator with Dual-drive Modulator

Article *in* IEEE Photonics Journal · December 2018

DOI: 10.1109/JPHOT.2018.2885783

6 authors, including:

Pengfei Zheng
Southeast University (China)
15 PUBLICATIONS **40** CITATIONS
SEE PROFILE

Jing Li
Southeast University (China)
8 PUBLICATIONS **8** CITATIONS
SEE PROFILE

Guohua Hu
Southeast University (China)
59 PUBLICATIONS **482** CITATIONS
SEE PROFILE

Binfeng Yun
Southeast University (China)
107 PUBLICATIONS **1,154** CITATIONS
SEE PROFILE

This article has been accepted for publication in a future issue of this journal, but has not been fully edited. Content may change prior to final publication. Citation information: DOI 10.1109/JPHOT.2018.2885783, IEEE Photonics Journal

Performances of Microwave Photonic Notch Filter Based on Microring Resonator with Dual-drive Modulator

Pengfei Zheng, Hong Hong, Jing Li, Guohua Hu, Binfeng Yun, Yiping Cui

Advanced Photonics Center, Southeast University, Nanjing 210096, China

Abstract: A tunable microwave photonic notch filter with ultra-high radio frequency rejection ratio is achieved by using a dual-drive Mach-Zender modulator and a microring resonator. In addition, we dedicated to clarify the mechanisms of the microwave photonic notch filters based on microring resonator under both over-coupled and under-coupled states and the performance differences between these two situations are investigated in detail. And the experimental results show that the cancellation microwave photonic notch filter with ultra-high RF rejection ratio can be achieved with both under-coupled and over-coupled microring resonators. Besides, a radio frequency rejection ratio exceeding 50 dB was achieved for microring resonator with optical extinction ratio of only 4 dB, where a 46 dB enhancement from optical to radio frequency response is obtained. Also, the bandwidth of the microwave photonic filter can tuned from 0.65 GHz to 2.2 GHz by adjusting the coupling ratio of the ring resonator. Meanwhile, by tuning the wavelength of the optical carrier, the filtering frequency can be tuned and a tuning range of about 25 GHz was achieved. The implementation is much simpler and more economical compared with previous reports and has great potential in monolithic integration of microwave photonic filters on chip.

Index Terms: Microwave photonics, Microring resonator, Optical filter, Integrated optics devices.

1. Introduction

Microwave photonics (MWP) offers new methods of the transmission and processing of radio frequency (RF) signals within optical domain with outstanding features as compared to the traditional microwave technologies [1]. Among the microwave photonics signal processing subsystems, microwave photonic filter is one of the typical components and has been broadly studied and applied. Compared with conventional electronic microwave filters, MWP filters have enormous advantages for their large frequency tuning ranges, reconfigurability and immunity to electromagnetic interference [2, 3]. It is widely used for numerous MWP applications and to form MWP signal processing systems with more complex functionalities including arbitrary waveform generation, optical beam-steering, analog-to-digital conversion, frequency measurement, etc. Among the MWP filters, the MWP notch (or bandstop) filter is adopted to eliminate the unwanted RF signals. Removing interferers in some radio systems, such as cognitive or ultrawideband radios, requires a very high notch peak rejection usually larger than 50 dB. And such applications require the MWP notch filter to have a high RF rejection ratio, a large frequency tuning range, and a tunable bandwidth in some cases. MWP notch filters are usually implemented via sideband filtering using the stimulated Brillouin scattering (SBS) effect [4, 5] or optical filters based on optical delay lines [6], fiber Bragg gratings [7, 8], Lyot loop filter [9], microring resonators (MRRs) [10-13]. Some studies combined the nonlinear effects with silicon [14] and silicon nitride (Si_3N_4) MRRs [15] to build MWP notch filters. Among these schemes, MWP notch filters based on the MRRs are of the biggest concern because MRRs can be monolithic integrated with other optical components conveniently. Furthermore, taking the advantage of electro-optic effect or thermo-optic effect, the extinction ratios and resonance frequencies of MRRs can be tuned easily and quickly. Hence, such MWP notch filters have tunability and reconfigurability that can be flexibly controlled.

A simple way to realize the MWP notch filter is combining the optical single sideband (OSSB) modulation with an optical filter such as MRR, taking the advantage of one-to-one mapping between the optical and radio frequency (RF) responses [3, 16]. However, the RF rejection ratio of such MRR based MWP notch filter is limited by the optical extinction ratio of the MRR, which is typically less than 30 dB due to the fabrication tolerances. To solve this problem, some MWP notch filters with ultra-high peak RF rejection ratios based on optical double sideband (ODSB) modulation by constructing destructive interferences between the mixing of the two optical sidebands with the optical carrier were proposed. There are two ways to achieve such destructive interference. One is to tailoring the amplitudes and phases of the two first order optical sidebands using special designed optical filters, such as two cascaded MRRs, under conventional ODSB modulation [17] which needs to precisely control the two rings simultaneously. This brings the difficulty in the operation of such MWP notch filter. Another way is to control the optical sideband suppression ratio (OSSR) of the modulated signal by varying the direct current (DC) biases of the modulator, such as the dual-parallel Mach-Zehnder modulator (DPMZM) [4]. However, there are three biases needed to be controlled in DPMZM when demonstrating the filter experimentally because the biases of the modulator will drift over time. That makes the control system of the MWP filter complex and costly. Besides, the effects of the over-coupled (OC) and under-coupled (UC) states of the MMR on the MWP notch filter are not clarified. Shahnia et. al. has proposed an MWP notch filter based on a bias-free phase modulator and a Fourier-domain optical processor (FD-OP) [18]. An improved solution is to use dual-drive Mach–Zehnder modulator (DDMZM), which has only one DC bias, instead of the DPMZM. Assisted with a fiber Bragg grating (FBG), an MWP notch filter based on DDMZM was proposed by Han et al. [19]. However,

This article has been accepted for publication in a future issue of this journal, but has not been fully edited. Content may change prior to final publication. Citation information: DOI 10.1109/JPHOT.2018.2885783, IEEE Photonics Journal

it is still hard to be monolithic integrated for both FD-OP and FBG.

Although the cancellation MWP notch filters based on MRRs have been widely studied, the former researches are mainly based on the nonlinear effects of MRRs or the over-coupled MRRs to achieve such MWP notch filters with ultra-high rejection ratios. In this paper, we dedicated to further clarify the mechanism of the MWP notch filter based on MRR under both OC state and UC state and investigated its properties. Hence, we proposed an MWP notch filter using a DDMZM assisted with a single MRR whose coupling state can be varied via thermo-optic effects. By controlling the DC bias of the DDMZM, the OSSR was manipulated to realize different modulation schemes. The phases of the mixing of the two optical sidebands and the optical carrier are depended on the interactions between the MWP link and the MRR. Thus, the MWP notch filters under different modulation schemes combined with MRR with different coupling states show different RF features. We have theoretically analyzed the mechanism of the proposed MWP notch filter and experimentally verified the filter's performances by employing an MRR based on Si_3N_4 platform. By optimizing the DC bias and the extinction ratio of MRR, an RF peak rejection ratio exceeding 55 dB under both OC and UC states have been obtained. Furthermore, we also found that a RF rejection ratio of 50 dB can be achieved with an MRR whose extinction ratio is as low as 4 dB. That means a twelve folds of rejection ratio enhancement were achieved when mapping from optical field to RF field. Moreover, by varying the frequency of the optical carrier, the filtering frequency of the MWP notch filter can be tuned with a tuning range over 25 GHz. Comparing with the scheme based on DPMZM, there is only one DC bias to be controlled in the DDMZM scheme, that makes it easier to implement a more stable MWP notch filter. And making use of the Si_3N_4 MRR, it is convenient to be integrated monolithically for the MWP system on chip in the future.

2. Principle and Theoretical Analyses

The schematic diagram of the proposed MWP notch filter is shown in Fig. 1. Via a 90° hybrid coupler, two RF signals with a phase difference of π/2 are generated by splitting the signal from the RF source. Then, the two RF ports of the DDMZM are driven by the two split RF signals, respectively. By controlling the DC bias of the DDMZM, we can modify the phase difference (denoted as $\Delta\varphi=\pi V_{DC}/V_{\pi,DC}$) between the optical signals of the two MZI arms.

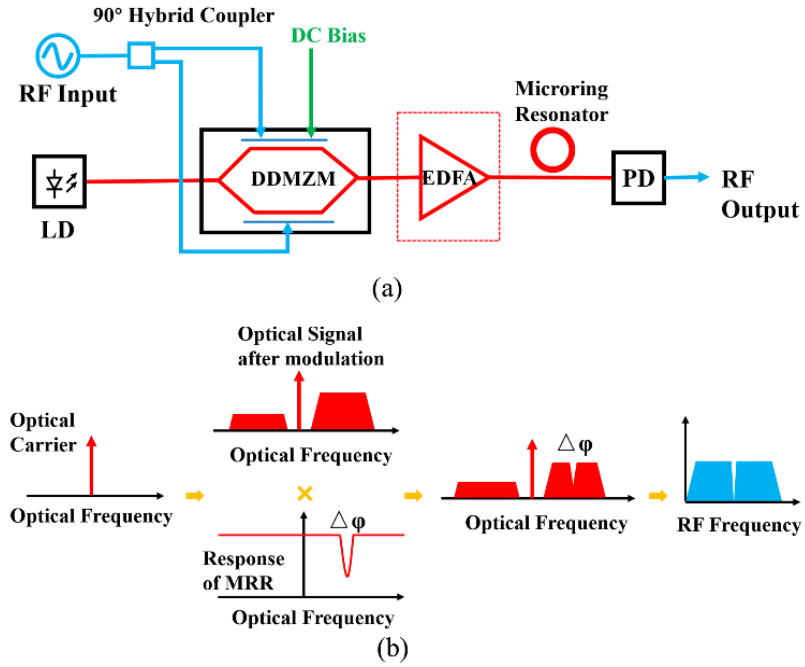

Fig. 1. (a) The scheme of the proposed MWP notch filter. (b) The principle diagram of the MWP notch filter in frequency domain.

The modulated optical signal can be expressed as [20]:

$$E(t)=\frac{1}{2}E_c\exp(i\omega_c t)\left\{\exp\left[i\frac{\beta}{\sqrt{2}}\cos(\omega_e t)+i\Delta\varphi\right]+\exp\left[i\frac{\beta}{\sqrt{2}}\cos\left(\omega_e t+\frac{\pi}{2}\right)\right]\right\} \quad (1)$$

Where β is the phase modulation index defined as $\beta=\pi V_{rf}/V_{\pi,rf}$, V_{rf} is the amplitude of the RF signal and $V_{\pi,rf}$ is the RF half-wave voltage of the DDMZM. ω_c and ω_e are the angular frequency of the optical carrier and RF signal, respectively. Making use of the Jacobi-Anger expansions, the electric fields of the optical carrier and two first order optical sidebands after the ODSB modulation are expressed as:

This article has been accepted for publication in a future issue of this journal, but has not been fully edited. Content may change prior to final publication. Citation information: DOI 10.1109/JPHOT.2018.2885783, IEEE Photonics Journal

$$E_0 = \frac{1}{2}E_c J_0\left(\frac{\beta}{\sqrt{2}}\right)\left[1+\exp(i\Delta\varphi)\right]\exp(i\omega_c t)$$
$$E_{-1} = \frac{1}{2}E_c J_1\left(\frac{\beta}{\sqrt{2}}\right)\left[\exp\left(i\Delta\varphi + i\frac{\pi}{2}\right)+1\right]\exp\left[i(\omega_c-\omega_e)t\right] \quad (2)$$
$$E_{+1} = \frac{1}{2}E_c J_1\left(\frac{\beta}{\sqrt{2}}\right)\left[\exp\left(i\Delta\varphi + i\frac{\pi}{2}\right)-1\right]\exp\left[i(\omega_c+\omega_e)t\right]$$

Where J_0 and J_1 are the Bessel functions of the first kind. According to Eq. (2), the amplitudes and phases of the optical carrier and the two first order optical sidebands can be adjusted by controlling the DC bias as shown in Fig. 2.

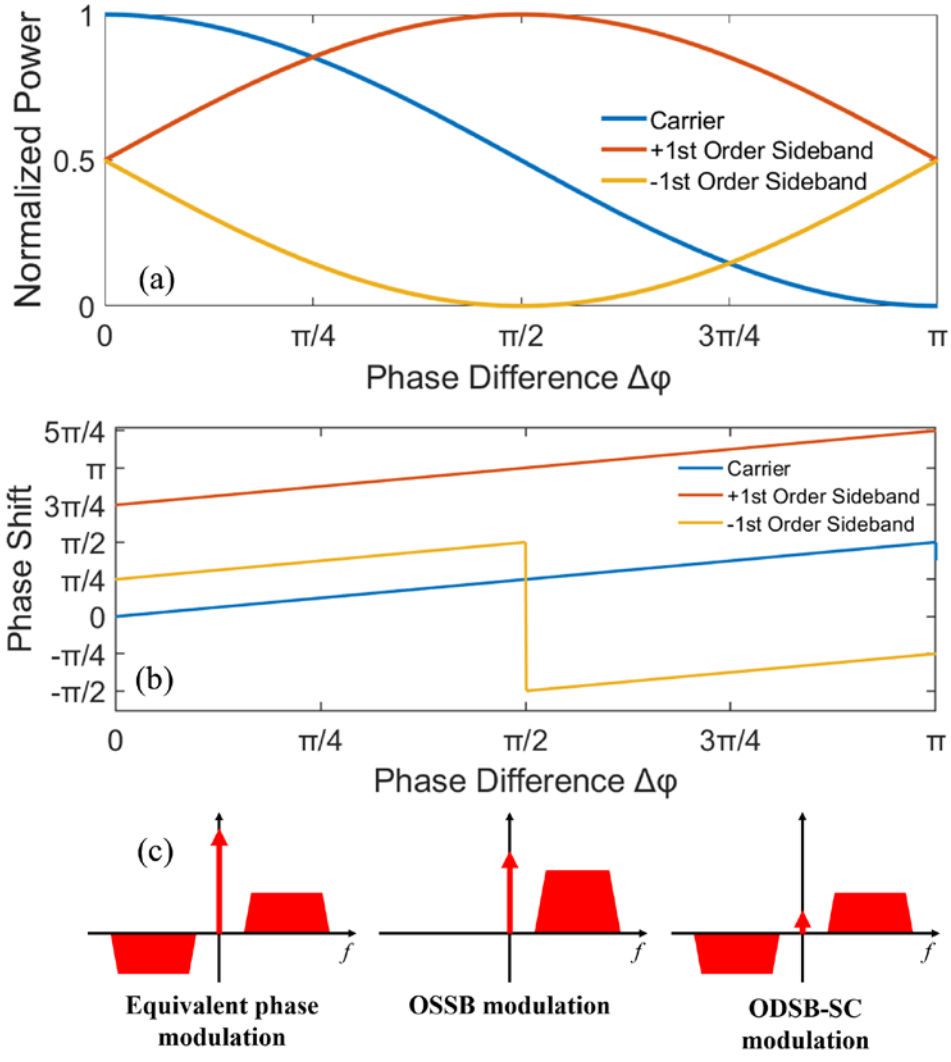

Fig. 2. (a, b) The amplitudes and phases of the optical carrier and the two first order optical sidebands vary with the DC bias of DDMZM. (c) The schematic diagrams of the three modulation schemes under the three specific DC bias.

As seen in Fig. 2, when the DC bias is tuned to obtain △φ=0, the two first order sidebands have the same amplitudes and the system is under the ODSB modulation (actually the equivalent phase modulation). When the DC bias is set as quadrature bias (△φ=π/2), an OSSB modulation is generated with the -1st order optical sideband suppressed completely and the OSSR tends to be infinity. Furthermore, when the DC bias is tuned to realize △φ=π, the optical carrier is suppressed, while the two first order sidebands have equal amplitudes. This condition is known as the double sideband with suppressed carrier (ODSB-SC) modulation.

First, the MWP link without optical filter is analyzed. The modulated signal is fed to the photodetector directly and the optical signal is converted into the RF photocurrent expressed as [20]:

$$I_{RF}(\omega_e) \propto E_0^{*}E_{+1} + E_0 E_{-1}^{*} \quad (3)$$

The two terms on the right side of Eq. (3) are the mixing products of the two first order sideband and the optical carrier, respectively. According to Eq. (2), the amplitudes and phases of the two mixing products are dependent on the phase differences induced by DC bias of the DDMZM. The mixing products of the two first order sideband and the optical carrier are illustrated in Fig. 3.

This article has been accepted for publication in a future issue of this journal, but has not been fully edited. Content may change prior to final publication. Citation information: DOI 10.1109/JPHOT.2018.2885783, IEEE Photonics Journal

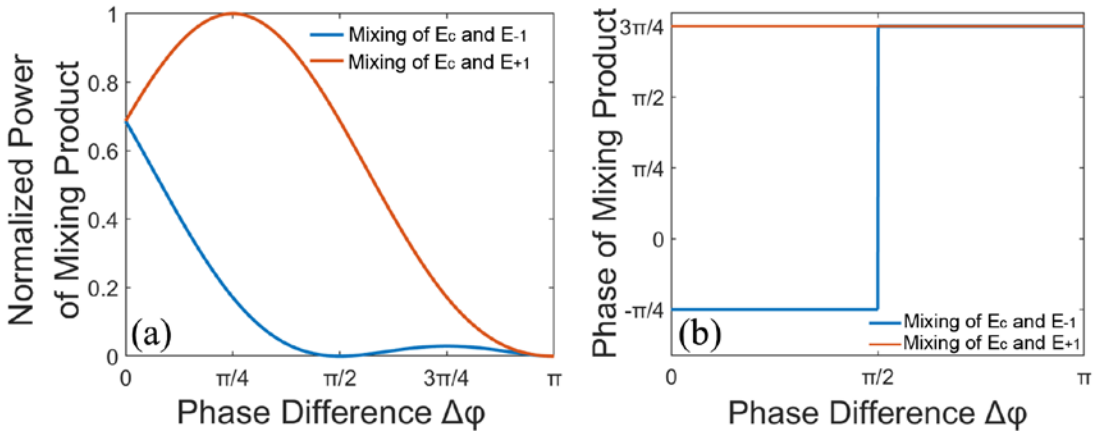

Fig. 3. The normalized powers (a) and phases (b) of the two mixing products vary with the phase difference induced by DC bias.

When △φ=0, the mixing products have a phase difference of π. In this case, the ODSB modulation has the same properties as a phase modulation [19]. When 0<△φ<π/2, the phase difference of the two mixing products is π, whereas, when π/2<△φ<π, the two mixing products have the same phase. As introduced in the last part, to obtain an MWP notch filter with ultra-high rejection, the mixing products of the two first order sidebands and the optical carrier should fulfill the cancellation condition, i.e., the mixing products should have the same amplitudes and should be antiphase. When 0<△φ<π/2, the antiphase condition is naturally met. Hence, by suppressing the mixing product with the larger amplitude without changing its phase, the cancellation condition can be matched. Meanwhile, when π/2<△φ<π, both amplitudes and phases of the mixing products should be controlled. So MRR under both the UC and OC states is adopted in this work to meet the amplitude and phase requirements of RF cancellation and construct the MWP notch filters.

The transfer function of the MRR is expressed as [21]:

$$H(\omega)=\frac{E_{out}}{E_{in}}=e^{i(\pi+\varphi)}\frac{a-te^{-i\phi(\omega)}}{1-ate^{i\phi(\omega)}} \tag{4}$$

Where *a* and *t* are the round trip transmission coefficient and the self-coupling coefficient of the MRR, respectively. ϕ is the round trip phase shift of optical signal traveling around the resonator, which is expressed as:

$$\phi(\omega)=\frac{\omega\cdot n_{eff}(\omega)L}{c} \tag{5}$$

Where ω is the angular frequency of light, c is the light speed in vacuum, L is the perimeter of the MRR, n_{eff} is the effective index of the waveguide mode, which is frequency dependent if the modal dispersion is taken into consideration. Among those parameters, *a* and *t* are the two vital parameters that determine the transmission spectra of the MRR. The MRR is inserted between the DDMZM and the photodetector to tailoring the optical sidebands of the modulated signal. Then, the processed optical signal is converted into RF photocurrent by the photodetector and is given by [20]:

$$I_{RF}(\omega_e)\propto E_0^{*}H(\omega_c)^{*}E_{+1}H(\omega_c+\omega_e)+E_0H(\omega_c)E_{-1}^{*}H(\omega_c-\omega_e)^{*} \tag{6}$$

Assuming that the resonance frequency of MRR is set at the -1st order sideband as ω_c-ω_e and the MRR has no effect on the optical carrier and the +1st order sideband, which means $H(\omega_c)=H(\omega_c+\omega_e)=1$. Then, Eq. (3) can be approximate as:

$$I_{RF}(\omega_e)\propto E_0^{*}E_{+1}+E_0E_{-1}^{*}H(\omega_c-\omega_e)^{*} \tag{7}$$

As known, when *a*<*t*, the MRR is under the UC state and a phase shift of zero is obtained at the resonance frequency. While for *a*>*t*, MRR is under the OC state, a π phase shift is existed at the resonance frequency. So according to Fig. (3), when 0<△φ<π/2, MRR under the UC state can meet the cancellation condition while MRR under OC state can fulfill the cancellation condition when π/2<△φ<π. Then by well tailoring the two first order optical sidebands, a cancellation MWP notch filter with ultra-high RF rejection ratio can be realized for the MRR working on both the UC and OC states theoretically. And experiments were carried out to demonstrate the cancellation MWP notch filters based on these two cases.

3.Experimental Results and Discussion

In this part, experiments were implemented to verify the proposed MWP notch filter without an EDFA and the properties of the MWP notch filter were investigated. An optical carrier from a tunable laser (Santac WSL-100), with 15 dBm output power, is modulated by a DDMZM (Fujitsu 40 Gbps LN Modulator) with an RF half-wave voltage of 3.8 V and optical insertion loss of 7 dB. The DDMZM is driven by the RF signals from a vector network analyzer (Agilent N5242A) with a 90° hybrid coupler (Krytar MODEL 3017360K). Then, the optical output of the DDMZM is sent to the Si_3N_4 MRR fabricated using the TriPleX™ low-loss waveguide technology. The structure of the MRR is shown in Fig. 4.

This article has been accepted for publication in a future issue of this journal, but has not been fully edited. Content may change prior to final publication. Citation information: DOI 10.1109/JPHOT.2018.2885783, IEEE Photonics Journal

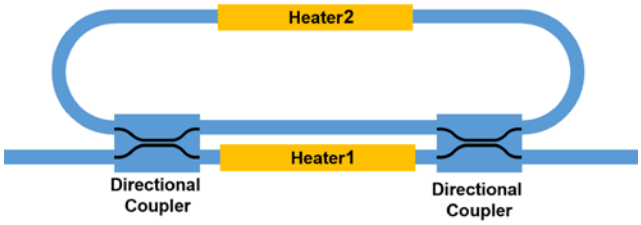

Fig. 4. The structure of the Si_3N_4 microring resonator with tunable extinction ratio.

As seen, there is a heater (Heater 1) over the MZI structure and the coupling coefficient *t* is tunable through thermo-optic effect of Si_3N_4 under different heating power. Hence, the extinction ratio of the MMR can be controlled. Another heater (Heater 2) was designed to realize the tuning of resonance frequency. The coupling loss between the fiber and the chip is about 5 dB by the edge coupling method. Then, a photodetector (Finisar XPDV2120RA), whose responsivity is 0.65 A/W, was adopted to retrieve the RF output signal. Finally, the RF output signal was sent back to the vector network analyzer to obtain the response of the system.

Before inserting the MRR into the MWP link, we have measured the optical transmission spectra using Agilent Lightwave measurement system (81640) and investigated the ERs of the MRR under different driven voltages applied upon the heater and we have figured out the OC state and the UC state of the MRR. The dependence of the ERs on the driven voltage is illustrated in Fig. 5(a). When the driven voltage is set near 10.4V, the maximum of ER of about 22 dB was obtained and the MRR is close to the critical coupling state. When the driven voltage is smaller than 10.4 V, the ER is positively correlated to the driven voltage and the MRR is under the OC state. While the ER is negatively correlated to the driven voltage that is larger than 10.4 V and the MRR is under-coupled. By fitting the spectra of the MRR under different driven voltages using Eq. (4) and Eq. (5), we obtained the relationship between the coupling efficient *t* and the driven voltage as shown in Fig. 5(b). We found that the round trip transmission coefficient *a* is about 0.95 (corresponding to the loss of the waveguide of about 0.48 dB/cm). When the driven voltage is 10.4 V, the coupling coefficient *t* is about 0.95 and the critical coupling condition (*a*=*t*) is fulfilled. Hence, by controlling the heater's driven voltage, the OC and UC states of the MRR can be easily switched. We should note that the dependence of coupling coefficient on the driven voltage will be affected by the fabrication deviation of the MRR. Hence, for different MRR, the properties of MRRs will be different our measured results here.

Then, by inserting the MRR into the MWP link, we have investigated the dependence of the RF spectra of the MWP notch filter on the DC bias of the DDMZM. A frequency sweep signal was generated to drive the DDMZM with an RF power of 0 dBm and the RF spectra responses were obtained. As is discussed in the last part, under different DC biases, the modulation schemes are different and can lead to the different RF spectra responses. Fig. 6 shows the RF spectra of the MWP notch filters with different DC biases of the DDMZM for the OC MRR and UC MRR.

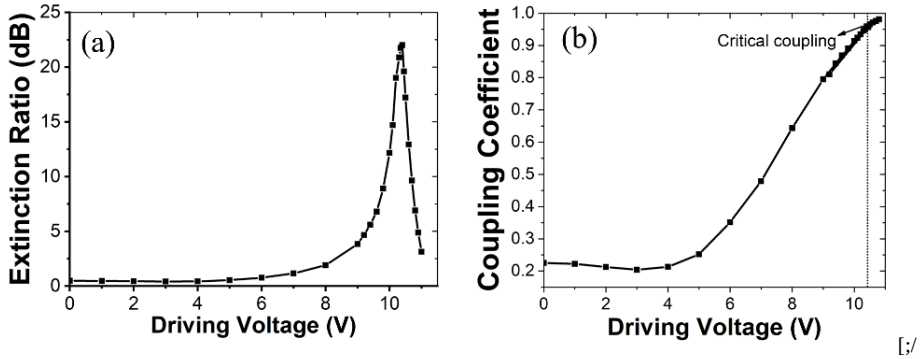

[;/

Fig. 5. (a) The ER of the MRR versus the driven voltage applied on the heater. (b) The dependence of the self-coupling coefficient *t* on the driven voltage (*a*=0.95).

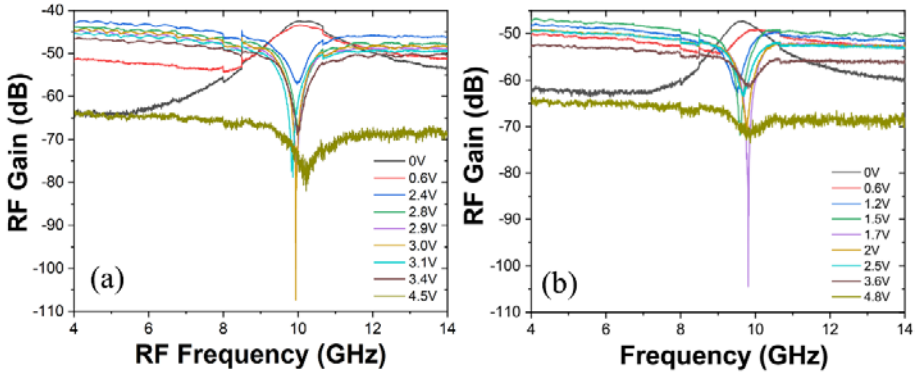

Fig. 6. The RF spectra of the MWP notch filters with different DC bias voltages of the DDMZM for the (a) OC MRR and (b) UC MRR.

This article has been accepted for publication in a future issue of this journal, but has not been fully edited. Content may change prior to final publication. Citation information: DOI 10.1109/JPHOT.2018.2885783, IEEE Photonics Journal

The frequency of the optical carrier is tuned to be 10 GHz larger as relative to resonance frequency of microring resonator. Thus, the filter frequency of the MWP notch filter is set as 10 GHz and the optical ER of the MRR is adjusted to be about 15 dB for both the UC and OC cases. Under both the OC and UC states of MRR, the MWP notch filter turns to be a bandpass filter when DC bias is near zero. In this case, the MWP link is under an equivalent phase modulation scheme [22]. When the bias voltage is set near the half-wave voltage V_{π} (about 4.8 V), the MWP link is under the ODSB-SC modulation scheme, and the RF response of the MWP notch filter has a low RF gain due to the suppression of the optical carrier. When the bias voltage is set about 3 V for the OC MRR and about 1.7 V for the UC MRR, the proposed MWP notch filter is optimized to obtain the largest rejection ratios over 55 dB and the cancellation conditions are fulfilled. We also measured the optical spectra under the OSSB modulation, the optimized modulation, the equivalent phase modulation, and the ODSB-SC modulation. The simulated and experimental results of the MWP notch filter and their corresponding optical transmission spectra before passing the MRR were illustrated in Fig. 7. The optical spectra were measured with a 10 GHz frequency RF signal applying on the DDMZM to modulate the optical signal. The experimental results match well with the simulation results. There is a deviation of RF gain between the experimental and simulation results especially at the high frequency. It is mainly resulting from the responsibility decreasing of the photodetector at the higher frequency. Also, the experimental filter frequencies are not aligned exactly at 10 GHz and leads to the frequency shift with respect to the simulation results.

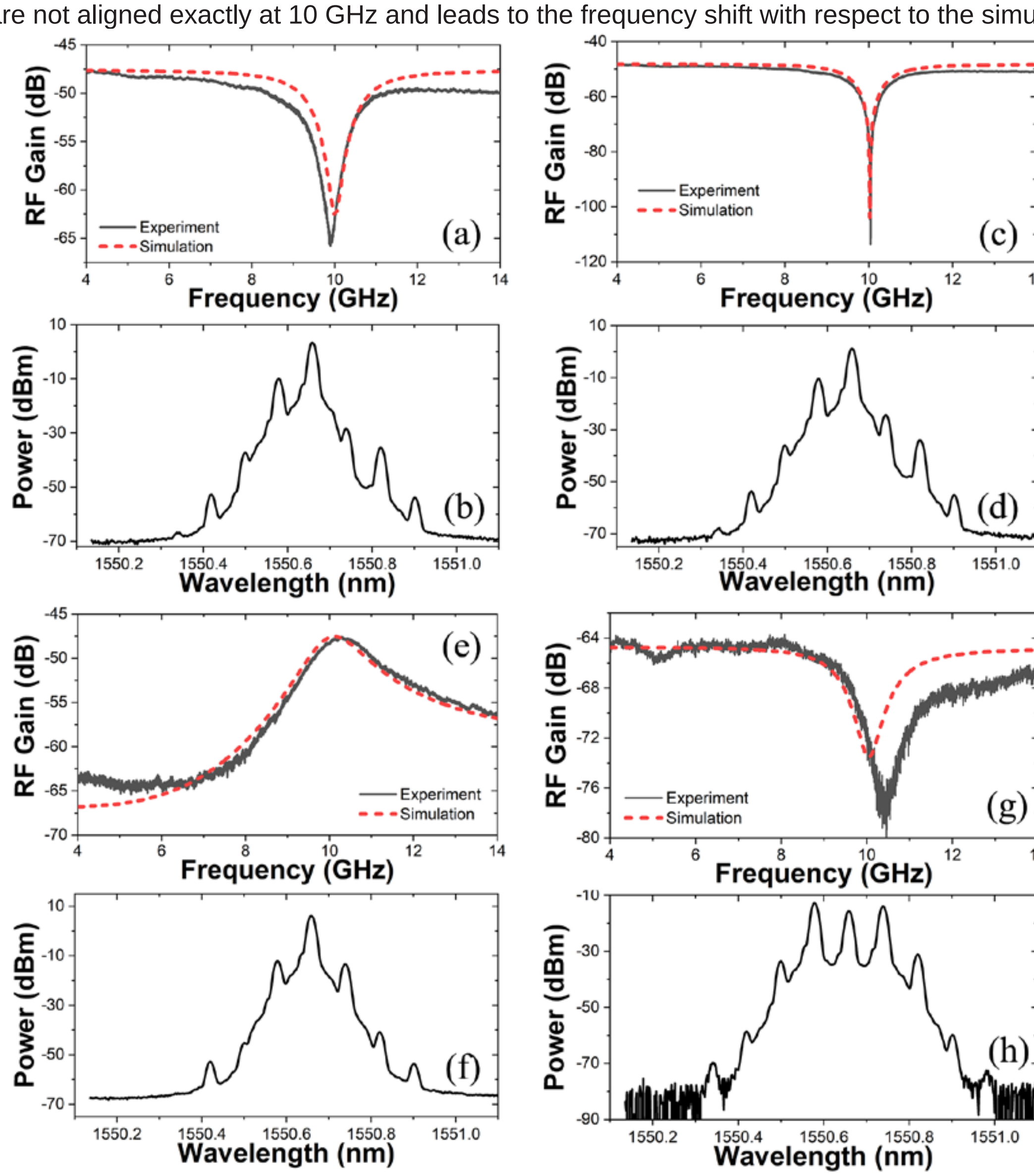

Fig. 7. The experimental and simulation results of the MWP notch filter and their corresponding modulated optical spectra before passing the MRR under (a, b) OSSB modulation, (c, d) the optimized modulation, (e, f) equivalent phase modulation, and (g, h) ODSB-SC modulation. An RF signal with 10 GHz frequency was applied on the DDMZM when measuring the optical spectra.

Then, we studied the impact of optical ER of the MRR on the RF response of the MWP notch filter. By tuning the heating power applied on the heater of MRR, the transmission coefficient *t* of MRR is modified to control the extinction ratio of MRR. By varying the extinction ratio of MRR from 4 dB to 22 dB and controlling the DC bias simultaneously, we have observed that the RF rejection ratio of the MWP notch filter can be achieved over 50 dB with an ER of only 4 dB under both the OC and UC states of MRR as illustrated in Fig. 8(a) and Fig. 8(b), respectively. When the optical ER is larger than 4 dB, the optimized RF rejection ratio can be further improved to 55 dB. Moreover, the RF gain is increasing when enlarging the ER

This article has been accepted for publication in a future issue of this journal, but has not been fully edited. Content may change prior to final publication. Citation information: DOI 10.1109/JPHOT.2018.2885783, IEEE Photonics Journal

under both OC and UC states. For the OC state, a smaller optical ER is corresponding to a larger DC bias needed for the cancellation condition. The mixing products of optical carrier and the two first order sidebands are decreasing as the increasing of DC bias, and results in the decreasing of the RF gain. While switching the MRR to the UC state, a smaller DC bias is required to realize a cancellation under a smaller optical ER, so the mixing products are increasing. However, the phases of the two mixing products are opposite at the non-resonance region of MRR. Hence, a more intense destructive interference between them is occurred and leads to the decreasing of the RF gain when the extinction ratio is small. Although the cancellation MWP notch filter can be realized with different ERs, when considering the RF gain of the filter, a larger optical ER is preferred. On the other hand, a larger optical ER requires a larger OSSR to match the two mixing products between optical carrier and the two first order optical sidebands, which is harder to be achieved in experimental implements.

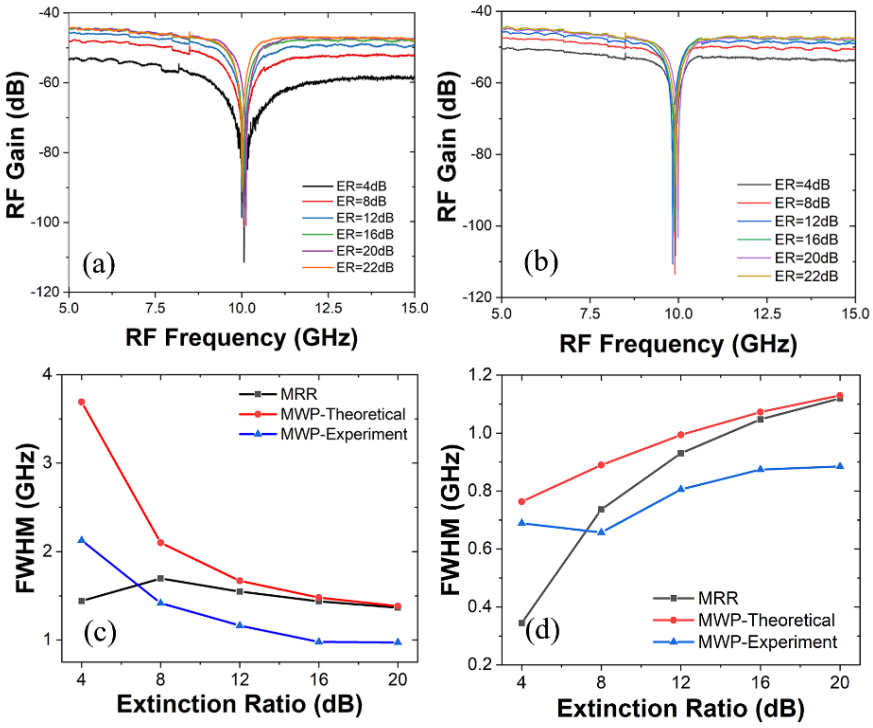

Fig. 8. The RF response under MRR with different extinction ratio, (a) for the OC state and (b) for the UC state. (c-d) the comparison of FWHM of MRR spectra and RF spectra of the proposed MWP notch filter with different ERs under OC and UC states.

We also noticed that the full width at half maximum (FWHM) of the MRR's resonance peak is also changed with the varying of extinction ratio. And the changing of the MRR's FWHM leads to the variation of MWP's FWHM. The FWHM is determined by the properties of the MRR and is related to the Q-factor of the MRR. Eq. (8) reveals the relationship between FWHM, Q-factor and the properties of the MRR [21].

$$FWHM = \frac{FSR}{\pi} \cdot \frac{1-at}{\sqrt{at}} \tag{8}$$

Where the FSR is the free spectra range of the MRR. The round trip transmission coefficient *a* and FSR are constants and the FWHM can be modified by controlling the coupling coefficient *t*. According to Eq. (8), the larger *t* is, the narrower FWHM will be. A comparison between the FWHM of MRR's optical spectra and RF spectra of the proposed MWP notch filter with different optical ERs is shown in Fig. 8(c) and Fig. 8(d). The theoretical and measured FWHMs of the RF spectra have the same trends as the FWHM of the optical spectra when tuning the ER of MRR. And the MWP notch filter based on UC MRR has a narrower FWHM than that of OC MRR theoretically and experimentally.

As known, the FWHM of MRR's optical spectrum is correlation to the Q-factor of the resonator as expressed by Eq. (9).

$$Q = \frac{f_0}{FWHM} \tag{9}$$

Where f_0 is the resonance frequency of the MRR. The Q-factor is formally defined as the ratio of the stored energy circulating inside the resonator to the energy lost per optical cycle. For an MRR optical filter, the energy loss in the resonator is determined by two factors: the round trip loss *a* of the resonator and the coupling loss from the resonator to the straight waveguide (that is $\sqrt{1-t^2}$ here). Eq. (9) can be derived from the formal definition of Q-factor [23]. The round trip loss *a* is a constant for a certain fabricated MRR. Thus, the energy loss of the resonator is determined by the coupling loss $\sqrt{1-t^2}$. Therefore, a larger self-coupling coefficient *t* leads to a smaller power loss and a larger Q-factor of the MRR and finally results in a narrower FWHM under both OC and UC states. The self-coupling coefficient *t* of UC state ($a<t$) is always larger than that of OC state ($a>t$), so the FWHM of UC state is always narrower than that of OC state as shown in Fig. 8(c) and Fig.

8(d). Besides, under the OC state, a larger ER corresponding to a larger *t* and leads to a narrower FWHM. While for the UC state, a larger ER corresponding to a smaller *t* and that results in a wider FWHM. On the other hand, the Q-factor has no impact on the frequency tuning range of the microwave photonic notch filter, which is determined by the FSR of MRR. By controlling *t* via modifying the heating power applied on the heater over the MRR, the bandwidth of the proposed MWP notch filter can be manipulated. According to the experimental results, the tuning range of the FWHM is from 0.65 GHz to 2.2 GHz. We also note that the filter frequencies under different ERs are not perfectly aligned at 10 GHz resulting from the thermal crosstalk of the heater, thus it needs a more precise control.

Then, we have focused on the tunability of the filter frequency of the MWP notch filter. As mentioned before, the frequency of the proposed MWP notch filter is equal to the frequency difference between the optical carrier and the resonance of the MRR. Thus, the frequency of the MWP notch filter can be tuned by adjusting either of them. Firstly, we adjust the optical carrier's frequency while keeping the resonance frequency of the MRR as a fixed value. The filter frequency of the proposed MWP notch filter tuned under OC and UC MRR are illustrated in Fig. 9(a) and Fig. 9(b). We have found that, when the frequency is larger than 2.5 GHz, a RF rejection ratio exceeding 55 dB can be achieved. Whereas, the RF rejection ratio and the RF gain will decrease when the filtering frequency is lower than 2.5 GHz. This is because as the optical carrier's frequency is getting close to the resonance frequency of the MRR, both the amplitude and phase of the optical carrier will be affected by the MRR and leads to the performance degradation of the MWP notch filter. Thus, the MWP notch filter has a lower limit of frequency tuning range and is not suitable for filtering the low frequency RF signals. Moreover, the FSR of the MRR studied in this work is 37.5 GHz, hence the filter frequency of the proposed MWP notch filter has a potential upper limit which is half of the FSR (18.75 GHz) theoretically. This upper limit can be extended to several hundred gigahertz by enlarging the FSR. When the optical carrier's frequency is set as half of the FSR larger or smaller than the resonance frequency of the MRR, both the two first order sidebands will be suppressed by the MRR and the cancellation condition is then broken. So in this frequency point, the rejection ratio of the MWP filter is much smaller than other frequencies. In addition, when the filter frequency is larger than 18.75 GHz while smaller than 37.5 GHz, the MWP notch filter can also work with an ultrahigh rejection ratio. However, there is a small notch at the frequency smaller than 18.75 GHz, which results from the suppression of -1st order sideband by the MRR. And for the UC state, the small notch turns to be a small passband but they have no significant impact on the passband. Hence, the MWP notch filter can be used in the frequency range of 2.5 GHz to 37.5 GHz. We also measured the MWP notch filter's responses with tuning the MRR's resonance frequency when keeping the optical carrier's frequency as a constant. Fig. 9(c) and Fig. 9(d) were the frequency responses under OC state MRR and UC state MRR, respectively. The results indicate that the tuning of optical frequency and the tuning of the MRR's resonance frequency have the same effect on the proposed MWP notch filter.

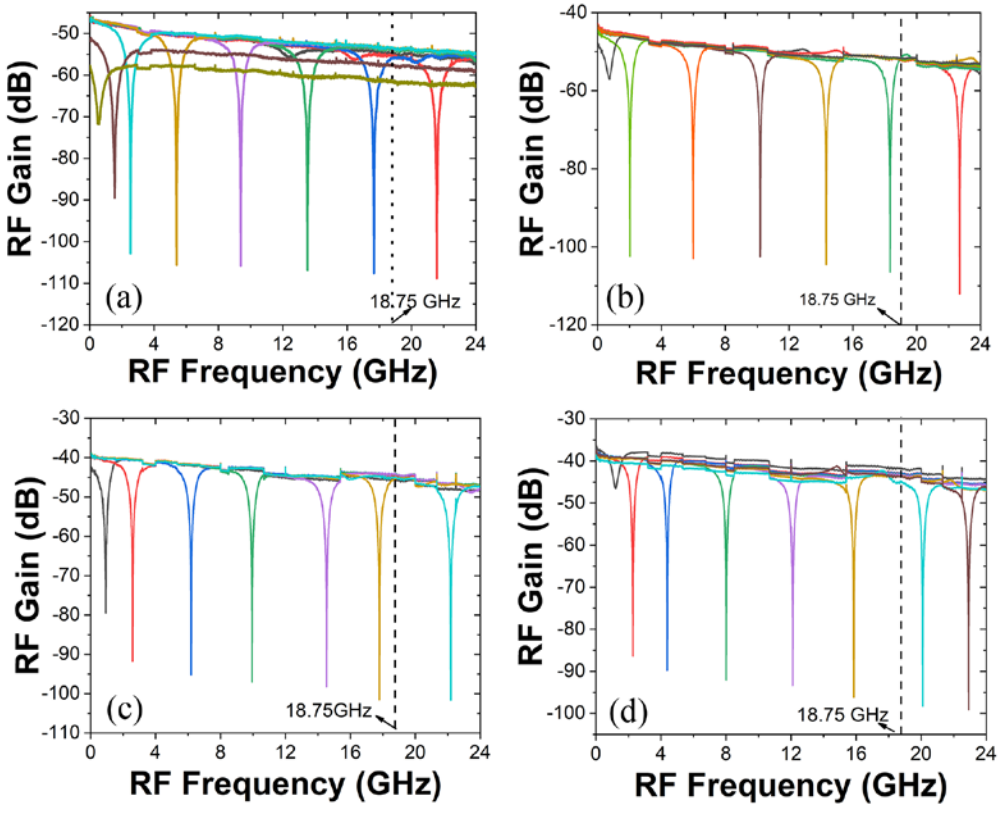

Fig. 9. The frequency responses of the MWP notch filter with tuning optical carrier's frequency under (a) OC state MRR and (b) UC state MRR. And The frequency responses of the MWP notch filter with tuning the resonance frequency of MRR under (c) OC state MRR and (d) UC state MRR when optical carrier's frequency was set as a constant.

Finally, we have worked on improving the RF gain of the passband of the filter. As seen in the RF spectra above, the RF

gain of the MWP notch filter is relatively low. The simplest way to solve this problem is to enlarging the optical power of the source or to amplify it. Besides, a low biasing technology was adopted to improve the RF gain with a low photocurrent and can also reduce the noise figure of the MWP link as is reported in Ref. [17]. However, the low biasing technology requires a much larger optical power and the link will suffer from a severe second order intermodulation distortion. In our experiment, an EDFA was inserted between the DDMZM and the MRR. The modulated signal was amplified for about 10 dB and the overall RF gain is improved for about 20 dB as is illustrated in Fig.10. However, the maximum optical power applied on the photodetector is limited by the saturation photocurrent of the photodetector. Thus, by adopting photodetector with a larger saturation current, the RF gain can be further improved.

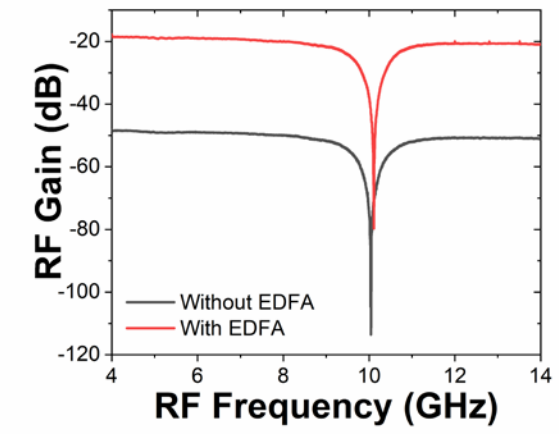

Fig. 10. The RF spectrum without EDFA and with EDFA, the RF gain is obviously improved.

4. Conclusion

In conclusion, we have proposed an MWP notch filter using the ODSB modulation with tunable OSSR realized by a DDMZM assisted by both OC MRR and UC MRR. By matching the OSSR with the optical extinction ratio of the MRR, an ultra-high peak RF rejection ratio can be achieved. The experimental results show that it can be optimized to obtain the RF rejection ratio exceed 55 dB. Moreover, an ultrahigh RF rejection of 50 dB can be reached when the optical extinction ratio of MRR is only 4 dB. And the FWHM can be tuned by controlling the self-coupling coefficient *t* of the MRR. Furthermore, by adjusting the wavelength of the optical carrier, the filter frequency can be tuned and a tuning range larger than 25 GHz was achieved. The structure of the proposed MWP notch filter is very simple, low cost and easy to implement. This work provides a new way for the applications of integrated MWP systems.

Acknowledgements

This work was supported by the Natural Science Foundation of Jiangsu Province under Grant BK 20161429.

References

[1] I. Gasulla, J. Capmany, J. Mora, et al. “Microwave Photonic Signal Processing”. J. Lightw. Technol., vol. 31, no. 4, pp. 571-586, 2013.
[2] J. Capmany, B. Ortega, D. Pastor, "A tutorial on microwave photonic filters", J. Lightw. Technol., vol. 24, no. 1, pp. 201-229, 2006.
[3] J.S. Fandifio, P. Muñoz, D. Doménech, J. Capmany, "A monolithic integrated photonic microwave filter", Nat. Photonics, vol. 11, no. 1, pp. 124-130, 2016.
[4] W. Zhang, R. A. Minasian, “Switchable and Tunable Microwave Photonic Brillouin-Based Filter”, IEEE Photon. J., vol. 4, no. 5, pp. 1443-1455, 2012.
[5] D. Marpaung, B. Morrison, M. Pagani, R. Pant, D. Choi, B. Luther-Davies, S. Madden, B. Eggleton, “Low-power chip-based stimulated Brillouin scattering microwave photonic filter with ultrahigh selectivity”, Optica, vol. 2, no. 2, pp. 76-83, 2015.
[6] J. Yao, "A fresh look at microwave photonic filters", IEEE Microw. Mag., vol. 16, no. 8, pp. 46-60, 2015.
[7] E. Xu, J. Yao, "Frequency- and notch-depth-tunable single-notch microwave photonic filter", IEEE Photon. Technol. Lett., vol. 27, no. 19, pp. 2063-2066, 2015.
[8] Y. P. Wang, M. Wang, W. Xia, X. Ni, "High-resolution fiber Bragg grating based transverse load sensor using microwave photonics filtering technique", Opt. Express, vol.24, no. 16, pp. 17960-17967, 2016.
[9] J. Ge, M. P. Fok, "Passband switchable microwave photonic multiband filter", Sci. Rep., vol. 5, 2015.
[10] A. Perentos, F. Cuesta-Soto, A. Canciamilla, B. Vidal, L. Pierno, N. S. Losilla, F. López-Royo, A. Melloni, S. Iezekiel, "Using a Si_3N_4 ring resonator notch filter for optical carrier reduction and modulation depth enhancement in radio-over-fiber links", IEEE Photon. J., vol. 5, no. 1, pp. 5500110, 2013.
[11] D. Zhang, X. Feng, X. Li, K. Cui, F. Liu, and Y. Huang, “Tunable and reconfigurable bandstop microwave photonic filter based on integrated microrings and Mach-Zehnder interferometer,” J. Lightw. Technol., vol. 31, no. 23, pp. 3668–3675, 2013.
[12] J. Dong, L. Liu, D. Gao, Y. Yu, A. Zheng, T. Yang, X. Zhang, "Compact notch microwave photonic filters using on-chip integrated microring resonators", IEEE Photon. J., vol. 5, no. 2, pp. 5500307, 2013.
[13] J. Palací, G. E. Villanueva, J. V. Galán, J. Martí, B. Vidal, "Single bandpass photonic microwave filter based on a notch ring resonator", IEEE Photon. Technol. Lett., vol. 22, no. 17, pp. 1276-1278, 2010.
[14] J. Wang, Y. Long. “All-optical tuning of a nonlinear silicon microring assisted microwave photonic filter: theory and experiment”. Opt. Exp., vol.23, no.14, pp.17758-17771, 2015.
[15] Y. Liu, D. Marpaung, A. Choudhary, B. J. Eggleton, "Lossless and high-resolution RF photonic notch filter", Opt. Lett., vol. 41, no. 22, pp. 5306-5309, 2016.

[16] X. Liu, Y. Yu, H. Tang, et al. “Silicon-on-insulator-based microwave photonic filter with narrowband and ultrahigh peak rejection”, Opt. Lett., vol. 43, no. 6, pp.1359-1362, 2018.
[17] Y. Liu, J. Hotten, A. Choudhary, B. J. Eggleton, and D. Marpaung, “All-optimized integrated RF photonic notch filter,” Opt. Lett., vol. 42, no.22, pp. 4631-4634, 2017.
[18] S. Shahnia, M. Pagani, B. Morrison, B. J. Eggleton, and D. Marpaung, “Independent manipulation of the phase and amplitude of optical sidebands in a highly-stable RF photonic filter”, Opt. Exp., vol. 23, no.18, pp. 23278-23286, 2015.
[19] X. Han, J. Yao, “Bandstop-to-Bandpass Microwave Photonic Filter Using a Phase-Shifted Fiber Bragg Grating”, J. Lightw. Technol., vol. 33, no. 24, pp. 5133-5139, 2015.
[20] P. S. Devgan, D. P. Brown, and R. L. Nelson, “RF performance of single sideband modulation versus dual sideband modulation in a photonic link,” J. Lightw. Technol., vol. 33, no. 9, pp. 1888–1895, 2015.
[21] W. Bogaerts, P. De Heyn, T. Van Vaerenbergh, K. De Vos, S. Kumar Selvaraja, T. Claes, P. Dumon, P. Bienstman, D. Van Thourhout, R. Baets, "Silicon microring resonators", Laser Photon. Rev., vol. 6, no. 1, pp. 47-73, 2012.
[22] M. Wang, J. Yao, "Optical vector network analyzer based on unbalanced double-sideband modulation", IEEE Photon. Technol. Lett., vol. 25, no. 8, pp. 753-756, 2013.
[23] J. Heebner, T. Ibrahim, R. Grover, “Optical micro-resonators: Theory fabrication and applications”, USA, NY, New York:Springer-Verlag, 2007.